Water Supply

Water Supply Vol 21 No 8, 4429 doi: 10.2166/ws.2021.187

Degradation of BTEX in groundwater by nano-CaO_2 particles activated with L-cysteine chelated Fe(III): enhancing or inhibiting hydroxyl radical generation

Xuecheng Sun [a], Meesam Ali [a,b], Changzheng Cui [a] and Shuguang Lyu [a,*]
[a] State Environmental Protection Key Laboratory of Environmental Risk Assessment and Control on Chemical Process, East China University of Science and Technology, Shanghai 200237, China
[b] Department of Chemical Engineering, Muhammad Nawaz Sharif University of Engineering and Technology, Multan 60000, Pakistan
*Corresponding author. E-mail: lvshuguang@ecust.edu.cn

XS, 0000-0001-5098-6427

ABSTRACT

The simultaneous oxidation performance of benzene, toluene, ethylbenzene, and xylene (BTEX) by nanoscale calcium peroxide particles ($nCaO_2$) activated with ferric ions (Fe(III)) and the mechanism of the enhancement of BTEX degradation by L-cysteine (L-cys) were investigated. The batch experimental results showed that the $nCaO_2$/Fe(III)/L-cys process was effective in the destruction of BTEX in both ultrapure water and actual groundwater. A proper amount of L-cys could enhance BTEX degradation due to the promotion of Fe(II)/Fe(III) redox cycles by the participation of L-cys, but an excessive presence of L-cys would cause inhibition. Adding 1.0 mM L-cys to the $nCaO_2$/Fe(III) system, the concentration of Fe(II) increased to 1.15 mM instantly. Simultaneously, the yield of HO• produced by the 1.0 mM L-cys-containing system was 0.066 mM at 180 min reaction, higher than that without L-cys (0.049 mM). When excess L-cys (5.0 mM) was added to the system, the amount of Fe(II) increased to 3.73 mM because excessive L-cys caused a large amount of Fe(III) in the system to be reduced. However, the yield of HO• decreased to 0.043 mM since excessive Fe(II) could conversely scavenge HO• to produce Fe(III) again. EPR tests and quenching results indicated that HO• was the dominant reactive species in the $nCaO_2$/Fe(III)/L-cys system. For the removal of BTEX, the optimal molar ratio of $nCaO_2$/Fe(III)/L-cys was 10.5/20/1 based on calculation by response surface methodology (RSM). Finally, the BTEX destruction pathway was proposed according to the detected intermediates by liquid chromatography–mass spectrometry (LC–MS).

Key words: BTEX, chemical oxidation, groundwater remediation, L-cysteine, nanoscale calcium peroxide particles

HIGHLIGHTS

- $nCaO_2$/Fe(III) system with L-cysteine (L-cys) was applied to remediate mixed contaminants.
- A suitable amount of L-cys promoted redox cycling (Fe(III) → Fe(II)).
- The mechanism of enhancing or inhibiting hydroxyl radical generation was investigated.
- Proposed BTEX destruction pathway in the $nCaO_2$/Fe(III)/L-cys system.
- $nCaO_2$/Fe(III)/L-cys system was recommended for BTEX-contaminated actual groundwater remediation.

INTRODUCTION

Mono-aromatic compounds (MACs), composed of one single benzene ring, exist in groundwater mainly as a result of accelerated industrialization (Dhanya 2019). Of these MACs, benzene, toluene, ethylbenzene, and xylenes (BTEX) are known to be relatively water-soluble and have carcinogenic and neurotoxic effects which can increase the risk of detrimental health effects (Stasik *et al.* 2015; Godin *et al.* 2020; Yang *et al.* 2020). It has been reported that BTEX are the most frequently detected aromatic hydrocarbons in contaminated groundwater in China, causing the rapid migration of BTEX pollution (Zhao *et al.* 2020). However, the groundwater in most MACs polluted sites is usually under anaerobic conditions where BTEX exhibits slower degradation kinetics and a more limited catabolic range in such environments (Stasik *et al.* 2015; Huang *et al.* 2017). Therefore, remarkable efforts are made toward *in situ* chemical oxidation (ISCO) to ensure BTEX degradation eventually to be broken off completely (Minetti *et al.* 2017; Ma *et al.* 2018; Xia *et al.* 2020).

Calcium peroxide (CaO_2), as an alternative oxidant for ISCO, has become a reassuring option in recent decades. CaO_2, compared with hydrogen peroxide (H_2O_2), has moderate longevity and can provide an aerobic condition for natural bacteria

(Khodaveisi *et al.* 2011). Most importantly, the released H_2O_2 from CaO_2 (the maximum amount of 0.47 g H_2O_2/g of CaO_2) can participate in the Fenton reaction and generate HO•, which are the dominant radicals for the pollutant degradation under aqueous conditions (Amina *et al.* 2018; Xue *et al.* 2018a, 2018b; Sun *et al.* 2019; Tang *et al.* 2020). At the same time, hydroperoxyl radical (HO_2•), superoxide radical (O_2^-•), singlet oxygen ($^1O_2$) and hydroperoxide anions (HO_2^-) can be generated as well in the CaO_2-based Fenton system (Ma *et al.* 2007; Zhang *et al.* 2015a, 2015b; Pan *et al.* 2018; Zheng *et al.* 2019). These reactive/reductive species can occur simultaneously in the Fenton or Fenton-like process and exhibit a different oxidizing/reducing capacity for diverse organic pollutants because of the high selectivity of these reactive species, such as O_2^-• and $^1O_2$ (Wang & Wang 2020). This means that the oxidizing capacity of the combined Fenton-like process varies with the different target pollutants. Moreover, nanoscale CaO_2 ($nCaO_2$) was synthesized and displayed better dispersion and transportation ability than commercial CaO_2 from our previous study, owing to its smaller particle size and larger surface area (Qian *et al.* 2013, 2016; Mosmeri *et al.* 2019; Ali *et al.* 2020; Sun *et al.* 2020). Therefore, $nCaO_2$ has shown great perspective and attraction to scientists and engineers. CaO_2, similar to the Fenton process, can be activated by transition metals (Lu *et al.* 2017). Some researchers reported the application of CaO_2 activated with ferrous ion (Fe(II)) for the remediation of groundwater contaminated by trichloroethylene (Zhang *et al.* 2015a, 2015b), carbon tetrachloride (Tang *et al.* 2018), tetrachloroethene (Jiang *et al.* 2019), and benzene (Xue *et al.* 2016). CaO_2 can be also activated with ferric ion (Fe(III)) through spontaneous superoxide/perhydroxyl-driven reactions as well as the regeneration of Fe(II) in the process (Zhang *et al.* 2017). However, that Fe(III) precipitation as ferric hydroxide ($Fe(OH)_3$) at neutral pH does not re-dissolve limits the application of the CaO_2/Fe(III) system (Zhou *et al.* 2017). Chelating agents have been employed to overcome the above-mentioned limitation by researchers. For instance, citric acid (CA), tartaric acid (TA), oxalic acid (OA), glutamic acid (Glu), and ethylenediaminetetraacetic acid (EDTA) were introduced to the iron activation of the Fenton process to prevent iron precipitation and accelerate iron recycling (Huang *et al.* 2016; Hu *et al.* 2018; Yuan *et al.* 2019; Bai *et al.* 2020). L-cysteine (L-cys), a sulfur-containing non-phenolic amino acid, also exhibits Fe(III)-reducing activity owing to the actively functional sulfhydryl group (–SH) (Lu *et al.* 2020; Ramos *et al.* 2020). A rapid transformation from Fe(III) to Fe(II) in the presence of L-cys can happen, and at the same time the oxidation of L-cys to cystine (Equation (1)) (Luo *et al.* 2016). Furthermore, weak coordination may occur between Fe(III) and the carboxyl group (–COOH) of L-cys (Li *et al.* 2016).

$$2\mathrm{Fe(III)} + 2\mathrm{HS{-}CH_2{-}\underset{\mathrm{COO^-}}{\underset{|}{CH}}{-}NH_3^+} \rightleftarrows \mathrm{NH_3^+{-}CH_2{-}\underset{\mathrm{COO^-}}{\underset{|}{CH}}{-}S{-}S{-}CH_2{-}\underset{\mathrm{COO^-}}{\underset{|}{CH}}{-}NH_3^+} + 2\mathrm{Fe(II)} + 2\mathrm{H^+} \quad (1)$$

However, Luo *et al.* (2016) reported that methylene blue removal increased with the concentration of L-cys up to 50 μM, and its removal decreased with further increase in L-cys concentration. Similarly, the degradation of sulfadiazine in an L-cys-Fenton system increased with the increase of L-cys usage at the beginning and decreased with much more L-cys addition (Lu *et al.* 2020). The consumption of HO• with excessive L-cys might be the primary reason. In order to clearly understand the performance of $nCaO_2$ in the L-cys-Fenton reaction on composite pollutant removal and to reveal the mechanism of the role of L-cys in this system, in this article, the evaluation of an L-cys chelating $nCaO_2$/Fe(III) system on BTEX removal was thoroughly investigated. The role of L-cys in the Fe(III)/Fe(II) cycle and the generation of HO• was confirmed. Finally, the application potential of the L-cys-Fenton system for BTEX removal in actual groundwater remediation implementation was demonstrated.

METHODS

Materials

Benzene (C_6H_6, 99.0%), toluene (C_7H_8, 99.0%), ethylbenzene (C_8H_{10}, 99.0%), xylenes (C_8H_{10}, 99.0%), hydrogen peroxide (H_2O_2, 30%wt), ferric sulfate ($Fe_2(SO_4)_3$, 99.0%), calcium chloride ($CaCl_2$, 96%), polyethylene glycol 200 (PEG 200, 99.0%), ammonia (NH_3•H_2O, 28%), sulfuric acid (H_2SO_4, 98%) and sodium hydroxide (NaOH, 96.0%) were purchased from Aladdin Reagent Co. Ltd (Shanghai, China). Tert-butanol ($C_4H_{10}O$, TBA, 99.0%), benzoic acid ($C_7H_6O_2$, BA, 99.5%), 5,5-dimethyl-1-pyrroline N-oxide ($C_6H_{11}NO$, DMPO, 99.0%) and L-cysteine ($C_3H_7NO_2S$, L-cys, 99.0%) were supplied from Shanghai Lingfeng Reagent Co. Ltd (Shanghai, China). The ultrapure water was provided by a Milli-Q water purification

system (Classic DI; ELGA, Marlow, UK). The actual groundwater from a well approximately 15 m deep below the surface (Songjiang, Shanghai, China) was used for preparing the actual BTEX contaminated solutions.

Preparation of $nCaO_2$

Briefly, $CaCl_2$ was utilized as the precursor and H_2O_2 was added drop-by-drop in the presence of the surface stabilizer PEG 200. The detailed preparation method of $nCaO_2$ can be found in the Supplementary Material, Text S1.

Experimental procedure

BTEX stock solutions (0.5 mM) were transferred into a 250 mL glass reactor. A magnetic stirrer was used to mix the solution homogeneously and the temperature was controlled at 20 °C. The test started immediately after introducing the predetermined dosages of Fe(III) and $nCaO_2$. At the desired intervals, 2.5 mL samples were withdrawn and transferred into headspace vials containing 1.0 mL methanol. The vials were sealed immediately and then analyzed by a gas chromatograph (GC) instrument.

Analytical methods

BTEX were analyzed by a GC coupling with a headspace auto-sampler, a flame ionization detector (FID), and an HP-5 column (30 m $\times$ 0.32 mm $\times$ 0.25 μm) as described in the Supplementary Material (Text S2). Benzoic acid (BA) was chosen as a probe to quantify the production of HO•. The calculated production of *p*-HBA by the reaction of BA and HO• has the conversion factor (5.87 $\pm$ 0.18) with the production of HO• in the system (Xue *et al.* 2018a, 2018b).

The samples were extracted at 3 min after the start of the reaction for the analysis of intermediates during BTEX degradation. An amount of 150 mL ethyl acetate was mixed with 150 mL of the reaction solution and rested for 5 min. The top layer ethyl acetate mixed solution was condensed to 1.5 mL by a rotary evaporator (N-1300D; Eyela, Japan). The condensed solution was filtered by an organic-phase filter and tested by liquid chromatography–mass spectrometry (LC–MS) (Q-Exactive plus; ThermoFisher, China) (Supplementary Material, Text S2). At 3 min after the start of the reaction, 1.0 mL samples were withdrawn from the reactor and mixed with 1.0 mL DMPO (20.0 mM) for 1 min, then the mixed samples were analyzed by electron paramagnetic resonance (EPR) (EMX-8/2.7; Bruker, USA) for the detection of reactive oxygen species. The DMPO-OH was monitored at the settings for the EPR spectrometer of center field (3,510.00 G), microwave frequency (9.79 GHz), and power (5.05 mW). Total organic carbon (TOC) was determined by using a TOC analyzer (LiquiTOC, Germany). The BTEX degradation test in the actual groundwater was carried out by replacing ultrapure water with actual groundwater. The natural organic matter (NOM) of the actual groundwater was determined by ion chromatography (ICS-1100; ThermoFisher, China).

A central composite design (CCD) based on the response surface methodology (RSM) was used for the analysis of BTEX degradation performance. The dosages of $nCaO_2$ and Fe(III) were coded as X_1 and X_2. The initial concentration of L-cys was considered as X_3, 21 groups of experiments were tested. The ranges of both X_1 and X_2 were set from 1.0 to 20.0 mM and the range of X_3 was set from 1.0 to 10.0 mM.

RESULTS AND DISCUSSION

Performance of BTEX removal in the $nCaO_2$/Fe(III)/L-cys system

A series of comparative tests were carried out to estimate the performance of BTEX degradation in the $nCaO_2$/Fe(III)/L-cys system in order to investigate the L-cys chelating effect. The control tests for BTEX removal were conducted without $nCaO_2$ or Fe(III) under the same conditions and the results showed the BTEX volatilization rate was less than 5.0%. The removal of BTEX was below 8.0% when only $nCaO_2$ or Fe(III) existed. This means that $nCaO_2$ or Fe(III) alone was not available to degrade BTEX. In the $nCaO_2$/Fe(III)/L-cys system, rapid BTEX destruction was observed within 10 min, and the destruction became slower in the remaining reaction time. The reaction was terminated at 180 min in this test (Figure S1).

The performance of BTEX degradation in various systems is presented in Figure 1(a). As can be seen from Figure 1(a), the degradation efficiencies of BTEX were 19.7%, 17.6%, 21.6%, and 17.7%, respectively, when $nCaO_2$ and Fe(III) co-existed, but had a significant improvement (91.3%, 91.4%, 92.3%, and 86.6% degradation efficiencies) when 1.0 mM L-cys was introduced into the system. This means that $nCaO_2$ activated with Fe(III) could simultaneously degrade the combined BTEX pollutants, and L-cys could effectively improve the degradation capacity of the system on BTEX removal. The degradation efficiency of BTEX in the $nCaO_2$/Fe(II) system was higher than that in the $nCaO_2$/Fe(III) system. A possible explanation might be that

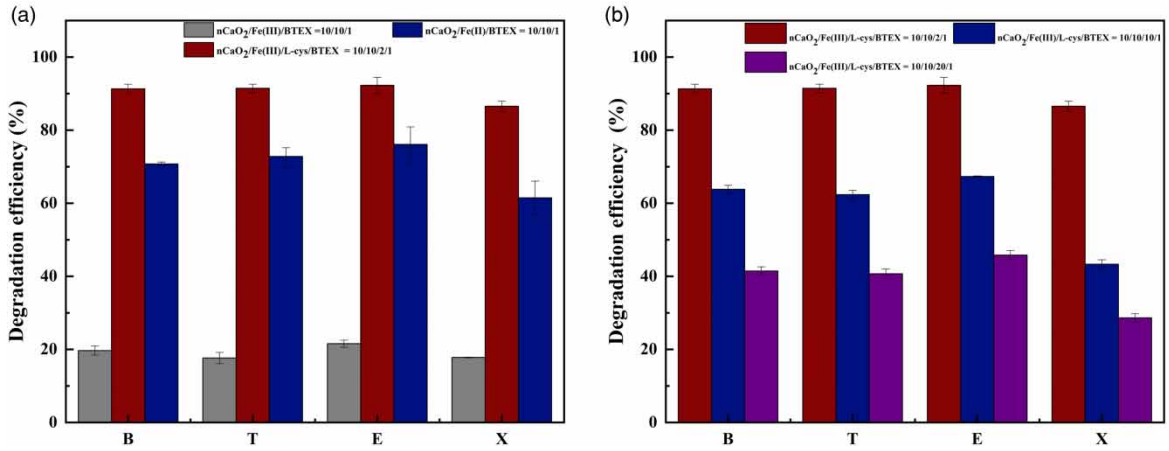

Figure 1 | BTEX removal performance in (a) various $nCaO_2$-based Fenton systems at 180 min and (b) $nCaO_2$/Fe(III)/L-cys system under different $nCaO_2$/Fe(III)/L-cys molar ratios at 180 min ([BTEX] = 0.5 mM, $nCaO_2$/Fe/BTEX = 10/10/1).

Fe(III) reacted with H_2O_2 released from $nCaO_2$-producing HO• radicals and Fe(II), and then Fe(II) catalyzed H_2O_2 to complete the Fenton reaction (Munoz *et al.* 2015). Matta *et al.* (2007) reported that minerals containing both Fe(III) and Fe(II) were more effective than Fe(III) oxides in the degradation of 2,4,6-trinitrotoluene. Giannakis *et al.* (2017) reported that Fe(II) salt was more efficient than Fe(III) on removing viruses from wastewater in the photo-Fenton process.

L-cys chelate-Fe(III) presented outstanding catalytic performance. Under the same molar ratio conditions, BTEX had higher removal in the $nCaO_2$/Fe(III)/L-cys system than those in the $nCaO_2$/Fe(III) and $nCaO_2$/Fe(II) systems (70.8%, 72.8%, 76.1%, and 61.5% removal of BTEX in the $nCaO_2$/Fe(II) system). However, with the addition of L-cys from 1.0 to 10.0 mM, the degradation efficiency of BTEX declined from 91.3%, 91.4%, 92.3%, and 86.6% to 41.4%, 40.7%, 45.8%, and 28.6%, respectively (Figure 1(b)). Therefore, it could be summarized that a proper amount of L-cys promoted the pollutant degradation ability of the $nCaO_2$/Fe(III) system, but excessive L-cys inhibited BTEX degradation. The excessive L-cys could compete for HO• with BTEX, leading to the decline of BTEX removal. This phenomenon of the consumption of HO• by excessive L-cys was also reported in a sulfadiazine degradation system (Lu *et al.* 2020).

To investigate the effect of the initial $nCaO_2$ or Fe(III) concentration on BTEX degradation, we established response surface methodology (RSM) models (Figure 2). When the initial L-cys concentration constant was made 1.0 mM, the degradation of BTEX increased along with the increase of $nCaO_2$ and Fe(III) concentrations. However, the increasing rates of xylenes by $nCaO_2$ and Fe(III) were higher than the others. This means that the degradation efficiency of xylenes was influenced by the initial concentration of $nCaO_2$ and Fe(III) more sensitively than benzene, toluene, or ethylbenzene. Overall, the influence of the BTEX degradation of factors X_1 and X_2 was the same, and a better degradation efficiency could be achieved at the same $nCaO_2$ and Fe(III) concentration. Making $nCaO_2$ or Fe(III) constant and increasing another concentration could not contribute to a better BTEX degradation. This result was also reported in the $nCaO_2$/Fe(II) system on BTEX removal (Sun *et al.* 2020). As the concentration of L-cys changed from 1.0 to 10.0 mM, more $nCaO_2$ and Fe(III) were needed to achieve the same BTEX removal (Figure S2 in the Supplementary Material). It also confirmed that excessive L-cys inhibited the system degradation ability for BTEX. The optimal molar ratio of $nCaO_2$/Fe(III)/L-cys was 10.5/20/1 based on the calculation by RSM. In subsequent studies, the molar ratios of 10/10/2/1 and 10/10/10/1 of $nCaO_2$/Fe(III)/L-cys were chosen to represent low and high L-cys concentrations to investigate the role of L-cys in the system.

Detection of free radicals in the $nCaO_2$/Fe(III)/L-cys system

In order to authenticate the occurrence and production of dominant radicals in the $nCaO_2$/Fe(III)/L-cys system, EPR tests were carried out using DMPO as the spin-trapping agent and the results are presented in Figure 3. In the $nCaO_2$/Fe(III) system, Fe(III) could not react directly with H_2O_2 to produce HO• and Fe(III) needs to be reduced to Fe(II) before reaction with H_2O_2 (Duesterberg *et al.* 2008; Fu *et al.* 2017). Therefore, the relative intensity of HO• in the $nCaO_2$/Fe(III) system was weak at 30 min of reaction. The concentration of Fe(II) increased significantly at 60 min, which strongly supported HO• production. However, the relative

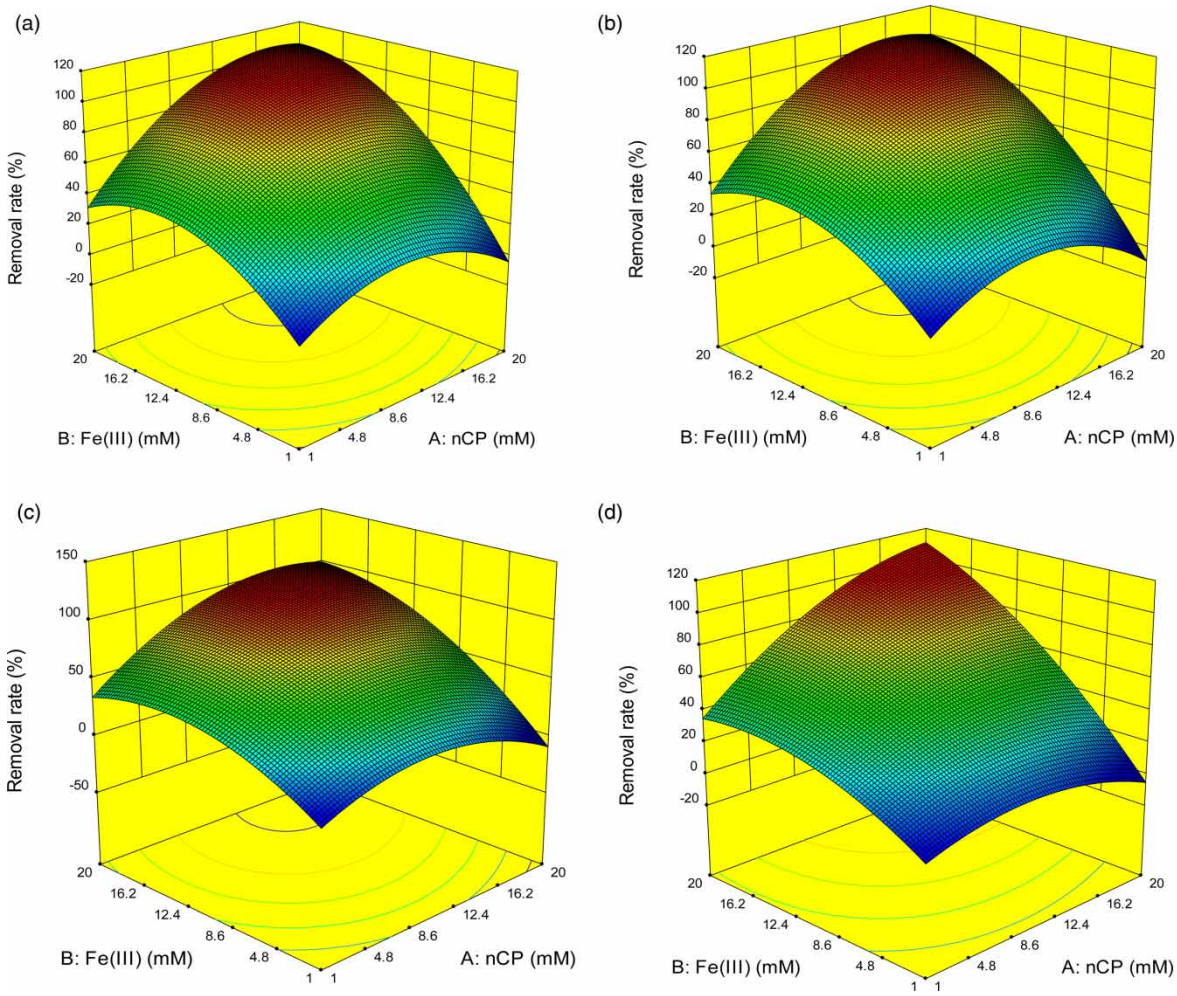

Figure 2 | Response surface of (a) B, (b) T, (c) E, (d) X for $nCaO_2$ (X_1) and Fe(III) (X_2) ([L-cys] = 1.0 mM).

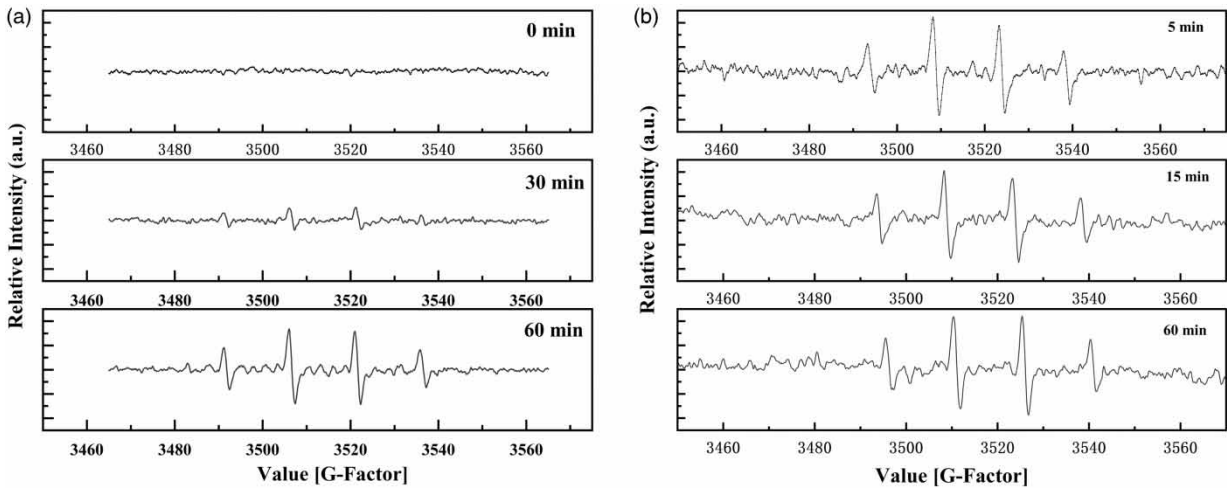

Figure 3 | EPR spectra of the (a) $nCaO_2$/Fe(III) system at the $nCaO_2$/Fe(III)/BTEX molar ratio of 10/10/1 and (b) $nCaO_2$/Fe(III)/L-cys system at the $nCaO_2$/Fe(III)/L-cys/BTEX molar ratio of 10/10/2/1 ([BTEX] = 0.5 mM).

intensity of HO• in the $nCaO_2$/Fe(III)/L-cys system was kept strong from 5 to 60 min. This means that the Fe(II) concentration in the $nCaO_2$/Fe(III)/L-cys system was high, in which Fe(II) could react with H_2O_2 and produce a large amount of HO• in a short time. There is a close relationship between the change of HO• and Fe(II)/Fe(III) redox cycles (Huang *et al.* 2020). It is deduced that the participation of L-cys promoted the Fe(II)/Fe(III) redox cycles in the $nCaO_2$/Fe(III)/L-cys system.

In order to further investigate the production of HO• in the $nCaO_2$/Fe(III)/L-cys system, BA (10 mM) was used as a probe to quantify the amount of HO• in the system. The production of HO• with the various dosages of $nCaO_2$/Fe(III)/L-cys/BTEX was calculated and is listed in Figure 4. The results showed that HO• accumulated rapidly within 60 min of the reaction. In the presence of L-cys, the system produced HO• at the beginning of the reaction, which was due to the rapid reduction of Fe(III) into Fe(II) by L-cys. During the first 30 min, the HO• accumulation rate was fast but slowed down after 30 min. However, in the system without L-cys, HO• accumulated gradually after 20 min of reaction but there was no further production after 60 min. It was noteworthy that the yield of HO• produced in the 1.0 mM L-cys-containing system was 0.066 mM at 180 min reaction, higher than that without L-cys (0.049 mM). The yield of HO• decreased to 0.043 mM with increasing the dosage of L-cys to 5 mM, and this explained why excessive L-cys inhibited BTEX degradation. Excessive L-cys caused a large amount of Fe(III) in the system to be reduced while excessive Fe(II) could conversely scavenge HO• to produce Fe(III) again (Equation (2)) (Xue *et al.* 2016). It was also reported that the rapid production of HO• would undergo HO• extinction reaction (Equation (3)), which made it difficult for HO• to react with other organic compounds in the system and hence limited the effectiveness of pollutant degradation (Yang *et al.* 2014).

$$Fe^{2+} + HO^{\bullet} \rightarrow Fe^{3+} + HO^{-} \quad (2)$$

$$HO^{\bullet} + HO^{\bullet} \rightarrow H_2O_2 \quad (3)$$

Effect of L-cys on Fe(III)/Fe(II) cycle in the $nCaO_2$/Fe(III) system

Iron species in the $nCaO_2$/Fe(III)/L-cys system were analyzed for understanding the effect of L-cys on the Fe(III)/Fe(II) cycle (Figure 5). In the system without L-cys (Figure 5(a)), a low concentration of Fe(II) (0.09 mM) was generated after 10 min and the maximum concentration of Fe(II) generated in the $nCaO_2$/Fe(III) system was only 0.16 mM at 20 min of reaction. The change of Fe(III)/Fe(II) could explain why the system began to accumulate HO• after 20 min as mentioned above. The Fe(III) in the system could not directly react with H_2O_2 to produce HO• and it has to be reduced to Fe(II) (Equations (4) and (5)) (Duesterberg *et al.* 2008). Since the reaction rate constant of Equation (5) ($k_{Fe(III),H_2O_2} = 2.0 \times 10^{-3}\ M^{-1}\ s^{-1}$) was smaller than that of Equation (4) ($k_{Fe(II),H_2O_2} = 7.6\ M^{-1}\ s^{-1}$), the accumulative rate of HO• was slow before there was

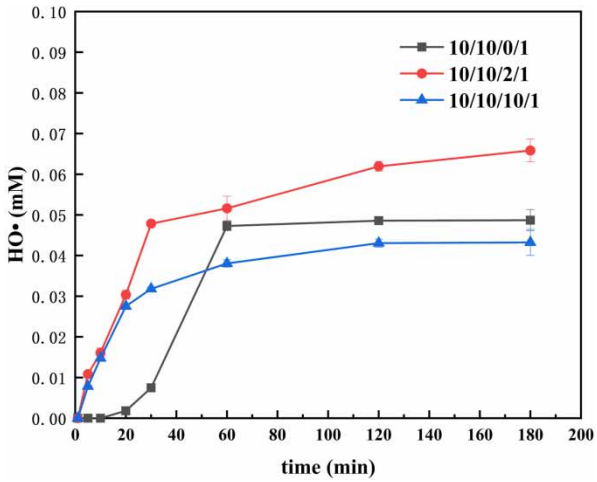

Figure 4 | The production of HO• with different dosages of chemicals in the $nCaO_2$/Fe(III)/L-cys/BTEX system ([BA] = 10 mM, [HO•] = 5.87 × [*p*-HBA], [BTEX] = 0.5 mM).

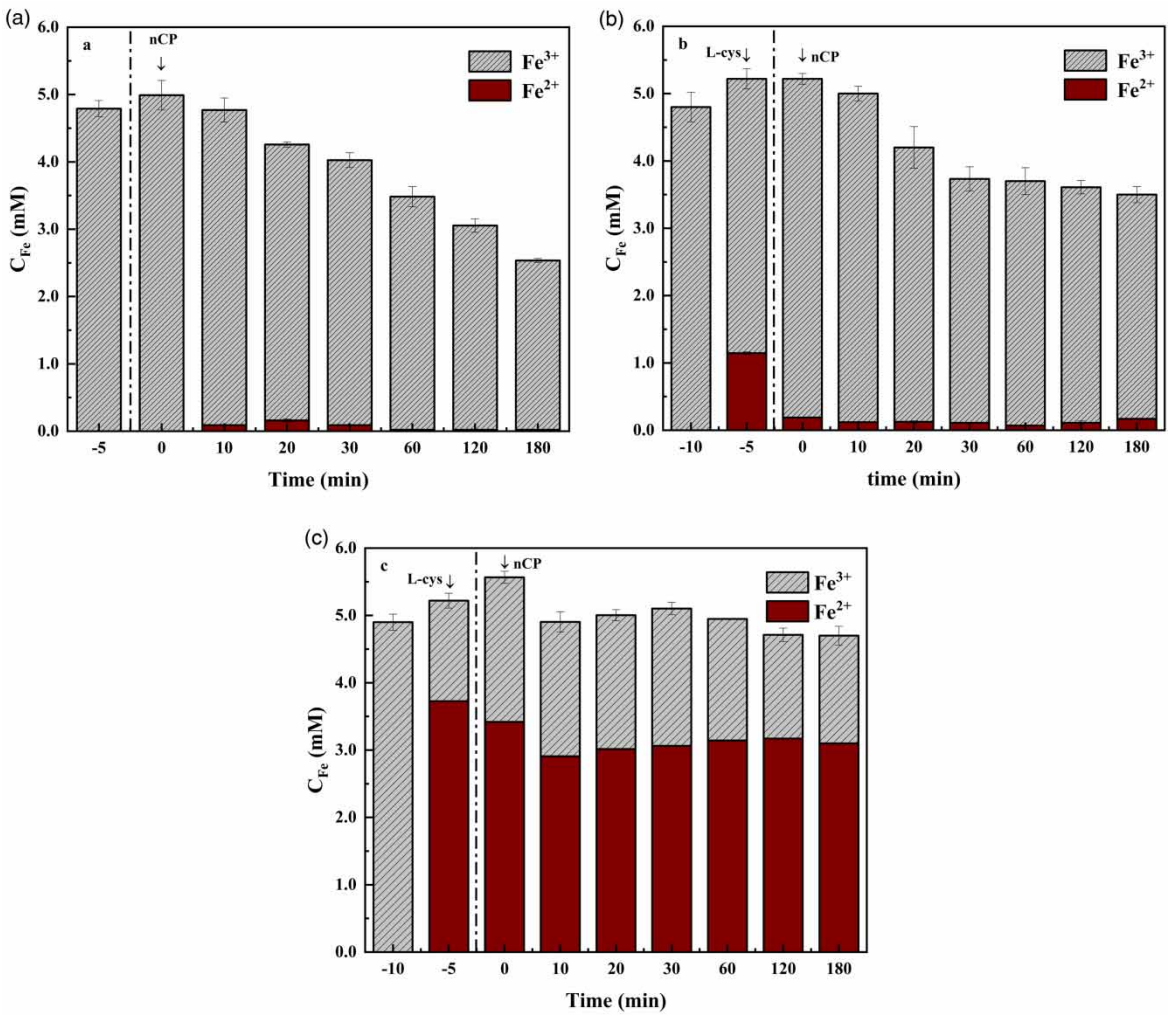

Figure 5 | The distribution of iron species in the $nCaO_2$/Fe(III)/L-cys/BTEX system at different $nCaO_2$/Fe(III)/L-cys/BTEX ratios of (a) 10/10/0/1, (b) 10/10/2/1, and (c) 10/10/10/1 ([BTEX] = 0.5 mM).

enough Fe(II) generation in the system (Li *et al.* 2020).

$$Fe^{3+} + H_2O_2 \rightarrow Fe - OOH^{2+} + H^+ \quad (4)$$

$$Fe - OOH^{2+} \rightarrow Fe^{2+} + HO_2^{\bullet} \quad (5)$$

However, by adding 1.0 mM L-cys into the $nCaO_2$/Fe(III) system, the concentration of Fe(II) increased to 1.15 mM instantly. During the reaction, the concentration of Fe(II) was changed within the range of 0.07 mM to 0.19 mM. When excessive L-cys (5.0 mM) was added to the system, the amount of Fe(II) increased to 3.73 mM (Figure 5(c)), and was still maintained high during the subsequent reactions. The L-cys could reduce Fe(III) to Fe(II), and Fe^{2+}(L-cys) and Fe^{2+}(L-cys)$_2$ complexes were generated simultaneously. The formations of Fe^{2+}(L-cys) and Fe^{2+}(L-cys)$_2$ complexes could increase the concentration of Fe(II) and strengthen the catalytic performance because the catalytic effect of Fe(II) was stronger than that of Fe(III) (Jiang *et al.* 2020). In addition, after 180 min reaction, the total soluble iron concentration in the $nCaO_2$/Fe(III) system was 2.53 mM (Figure 5(a)). However, the total iron concentration increased to 3.50 mM and 4.71 mM when the dosage of L-cys was 1.0 mM and 5.0 mM, respectively (Figure 5(b) and 5(c)), and this was simply due to less formation of precipitation after adding L-cys into the system (Ye *et al.* 2020).

The mechanism of BTEX destruction

Tert-butanol (TBA) was selected as HO• scavenger to evaluate the dominant radicals in the $nCaO_2$/Fe(III)/L-cys system due to TBA having a high reaction rate with HO• ($k_{HO\bullet} = 5.2 \times 10^8\ M^{-1}s^{-1}$) (Cai *et al.* 2020). The results showed that BTEX removal was significantly inhibited when TBA was added (Figure 6). BTEX removal at 180 min in the $nCaO_2$/Fe(III)/L-cys system decreased from 91.3%, 91.4%, 92.3%, and 86.6% to 9.5%, 9.7%, 11.8%, and 9.1%, respectively, which, along with the EPR test results, indicated that HO• was the dominant reactive species in the $nCaO_2$/Fe(III)/L-cys system.

The intermediates during BTEX degradation were analyzed by LC–MS and the possible BTEX destruction pathway is proposed in Figure 7. For the benzenoid compounds, the benzene-ring could be attacked by HO• to form various intermediate phenols (Gligorovski *et al.* 2015), such as $C_6H_6O_3$ ($m/z = 126$), $C_7H_8O_3$ ($m/z = 140$), and $C_8H_9O_3$ ($m/z = 153$). Further, HO• led to benzene-rings opening and formed short-chain alkanes and alkenes, such as $C_5H_7O_4$ ($m/z = 131$), $C_4H_5O_3$ ($m/z = 101$), and $C_3H_5O_3$ ($m/z = 89$). These intermediates and aromatic compounds were attacked by HO• and finally were completely mineralized. Since HO• are non-selective oxidation radicals, the reaction rate constants between organic compounds

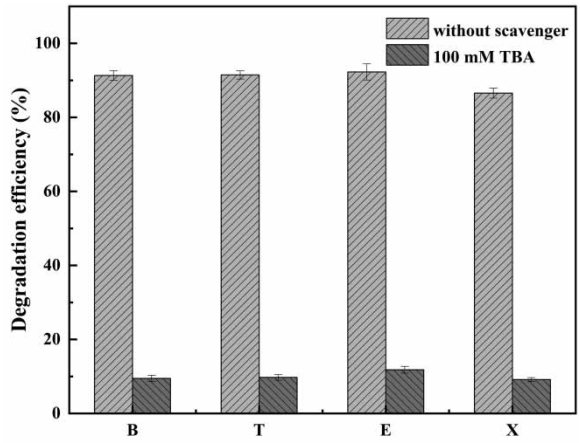

Figure 6 | Effect of scavenger on BTEX degradation in the $nCaO_2$/Fe(III)/L-cys system ([BTEX] = 0.5 mM, [TBA] = 100 mM).

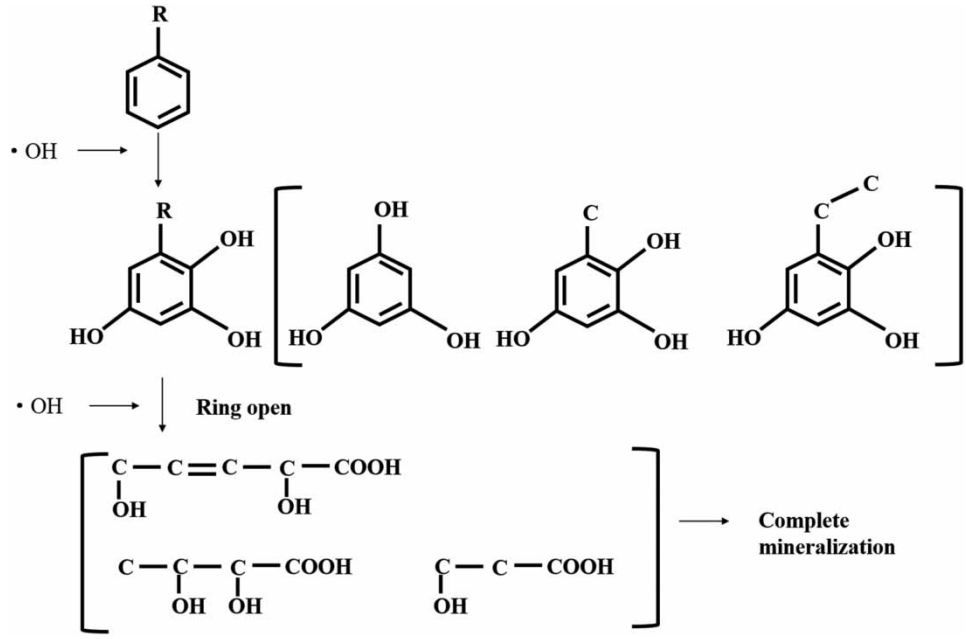

Figure 7 | Proposed BTEX destruction pathway in the $nCaO_2$/Fe(III)/L-cys system.

containing intermediates and HO• are in a range of 10^9–10^{10} $M^{-1}s^{-1}$ (Xue *et al.* 2018a, 2018b). In this study, although BTEX removal exceeded 90% in the $nCaO_2$/Fe(III)/L-cys system, most intermediates in the reaction belonged to aromatic compounds. The toxicity during BTEX degradation and the related study need to be investigated in our future research.

Performance of BTEX removal in the actual groundwater

To investigate the effect of the $nCaO_2$/Fe(III)/L-cys system on BTEX removal in the actual groundwater, the tests were carried out using the actual groundwater instead of ultrapure water (Figure 8). The characteristics of the actual groundwater used in the tests are listed in Table 1. As to the results, only 12.1%, 13.4%, 15.6%, and 14.0% BTEX had been removed when $nCaO_2$ and Fe(III) existed at the $nCaO_2$/Fe(III)/BTEX molar ratio of 10/10/1. When 1.0 mM L-cys was added into the system, the removal rate of BTEX increased to 56.3%, 57.2%, 59.3%, and 53.2%, which was about 60% of the degradation rate compared with ultrapure water. The main reason was that the initial pH of the actual groundwater was nearly neutral (7.31 ± 0.2) and it had a strong buffer capacity which could maintain the pH without large change during the reaction. As the Fenton reaction is affected by the pH of the solution (Sarmento *et al.* 2016), the effect of initial solution pH on BTEX degradation was investigated and the results are shown in the Supplementary Material (Figure S3a). At pH 6.2, the system had the highest BTEX degradation efficiency and the degradation ability was inhibited under acidic and/or alkaline conditions. Besides, the existence of Cl^-, HCO_3^-, SO_4^{2-} and the natural organic matter (NOM), humic acid (HA) being a typical NOM, were not conducive to the degradation of BTEX (Figure S3b). The results showed that HCO_3^- had the most significant effect on

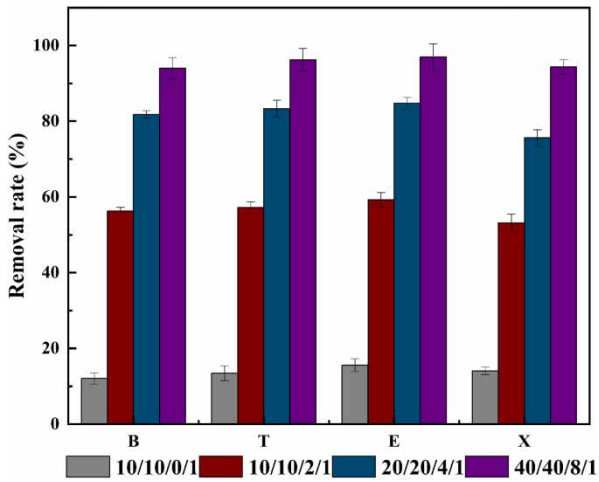

Figure 8 | BTEX removal performance in the actual groundwater in $nCaO_2$/Fe(III)/L-cys systems at various $nCaO_2$/Fe(III)/L-cys/BTEX molar ratios at 180 min ([BTEX] = 0.5 mM).

Table 1 | Characteristics of the actual groundwater used in experiments

Parameter	Units	Value
pH		7.31 ± 0.2
Total organic carbon (TOC)	mg L^{-1}	11.35 ± 0.5
Cl^- concentration	mg L^{-1}	127.5 ± 1.2
HCO_3^- concentration	mg L^{-1}	91.3 ± 1.5
NO_3^- concentration	mg L^{-1}	1.1 ± 0.1
SO_4^{2-} concentration	mg L^{-1}	62.7 ± 3.5
Ca^{2+} concentration	mg L^{-1}	126.0 ± 4.0
Mg^{2+} concentration	mg L^{-1}	27.3 ± 2.6
BTEX concentration	mg L^{-1}	Not detected

BTEX degradation, with a 52.7% reduction in degradation efficiency. The inhibitory effect of HCO_3^- on BTEX degradation in the $nCaO_2$/Fe(III)/L-cys system could be speculated as being for two reasons: the increasing of the solution pH and the scavenging effect of HO• (Zhang *et al.* 2015a, 2015b). HA had little effect on BTEX degradation. Therefore, under the actual groundwater conditions, the degradation ability of the $nCaO_2$/Fe(III)/L-cys system was inhibited. Encouragingly, the removal rates of BTEX were promoted to 94.0%, 96.2%, 97.1%, and 94.3%, respectively, when the molar ratio of $nCaO_2$/Fe(III)/L-cys/BTEX increased to 40/40/8/1. Increasing the molar ratio of $nCaO_2$/Fe(III)/L-cys/BTEX was an effective way to overcome the adverse effects caused by the complex of the actual groundwater. The degradation efficiencies of BTEX were 81.8%, 83.3%, 84.8%, and 75.6%, respectively, when the $nCaO_2$/Fe(III)/L-cys/BTEX molar ratio was 20/20/4/1. Increasing the molar ratio to 40/40/8/1, the degradation efficiencies of BETX increased to 94.0%, 96.2%, 96.9%, and 94.3%, respectively. Although the molar ratio of $nCaO_2$/Fe(III)/L-cys/BTEX doubled, the degradation efficiency only increased in the range of 12.1%–18.7%. Considering the remedial cost, the optimal ratio of $nCaO_2$/Fe(III)/L-cys/BTEX was set as 20/20/4/1 in the practical groundwater treatment. The agent cost of treating 1 m^3 of groundwater was calculated to be $28.50 at the optimal molar ratio condition. The above results strongly demonstrated that the $nCaO_2$/Fe(III)/L-cys system has broad application prospects in the actual groundwater environment for BTEX removal.

CONCLUSION

In this study, BTEX removal in the $nCaO_2$/Fe(III)/L-cys system was performed and the results showed that the $nCaO_2$/Fe(III)/L-cys technique could be efficient in destruction of BTEX in both ultrapure water and actual groundwater. A proper amount of L-cys could promote the degradation ability of the $nCaO_2$/Fe(III) system because the participation of L-cys accelerated the Fe(III)/Fe(II) redox cycles, but excessive L-cys inhibited them. After adding 1.0 mM L-cys into the $nCaO_2$/Fe(III) system, the concentration of Fe(II) increased to 1.15 mM instantly. Simultaneously, the proper concentration of L-cys was conducive to the accumulation of HO•. The yield of HO• produced in the 1.0 mM L-cys-containing system was 0.066 mM, higher than that without L-cys (0.049 mM) at 180 min. When excessive L-cys (5.0 mM) was added to the system, the amount of Fe(II) increased to 3.73 mM, however, the yield of HO• decreased to 0.043 mM. Excessive L-cys caused a large amount of Fe(III) in the system to be reduced, and excessive Fe(II) could in turn scavenge HO• to produce Fe(III). The optimal molar ratio of $nCaO_2$/Fe(III)/L-cys was 10.5/20/1 based on calculation by RSM. EPR tests and quenching results indicated that HO• was the dominant reactive species in the $nCaO_2$/Fe(III)/L-cys system. According to the detected intermediates by LC-MS, the BTEX destruction pathway was proposed. For these benzenoid compounds, the benzene-ring was attacked by HO• to form various intermediate phenols, and further HO• led to benzene-rings opening to form short-chain alkanes and alkenes and finally being completely mineralized. Under the actual groundwater conditions, the $nCaO_2$/Fe(III)/L-cys system has broad application prospects in the actual groundwater environment for BTEX removal. Considering the remedial cost, the optimal molar ratio of $nCaO_2$/Fe(III)/L-cys/BTEX was set as 20/20/4/1.

ACKNOWLEDGEMENTS

This study was financially supported by the National Key R&D Program of China (No. 2018YFC1803304) and the National Natural Science Foundation of China (No. 41977164).

ETHICAL APPROVAL

The authors confirm that this manuscript has not been previously published as a whole or part and it is not under consideration by any other journal.

CONSENT TO PARTICIPATE

All authors have approved the content and consent to submit it.

CONSENT TO PUBLISH

All authors have approved the content and consent to publish it.

AUTHORS' CONTRIBUTIONS

Xuecheng Sun: Conceptualization, Methodology, Investigation, Writing – Original Draft, **Meesam Ali:** Validation, Formal analysis, Writing – Review & Editing, **Changzheng Cui:** Resources, Visualization, **Shuguang Lyu:** Conceptualization, Writing – Review & Editing, Supervision.

DATA AVAILABILITY STATEMENT

All relevant data are included in the paper or its Supplementary Information.

REFERENCES

Ali, M., Shan, A., Sun, Y., Gu, X. G., Lyu, S. G. & Zhou, Y. B. 2020 Trichloroethylene degradation by PVA-coated calcium peroxide nanoparticles in Fe(II)-based catalytic systems: enhanced performance by citric acid and nanoscale iron sulfide. *Environmental Science and Pollution Research* **28** (3), 3121–3135.

Amina, Si, X. Y., Wu, K., Si, Y. B. & Yousaf, B. 2018 Synergistic effects and mechanisms of hydroxyl radical-mediated oxidative degradation of sulfamethoxazole by Fe(II)-EDTA catalyzed calcium peroxide: implications for remediation of antibiotic-contaminated water. *Chemical Engineering Journal* **353**, 80–91.

Bai, Y., Wu, D., Wang, W., Chen, P., Tan, F., Wang, X., Qiao, X. & Wong, P. K. 2020 Dramatically enhanced degradation of recalcitrant organic contaminants in MgO_2/Fe(III) Fenton-like system by organic chelating agents. *Environmental Research* **192**, 110242.

Cai, M. Q., Zhang, Y., Dong, C. Y., Wu, W. T., Wang, Q., Song, Z. J., Shi, Y. J., Wu, L. G., Jin, M. C., Dionysiou, D. D. & Wei, Z. S. 2020 Manganese doped iron–carbon composite for synergistic persulfate activation: reactivity, stability, and mechanism. *Journal of Hazardous Materials* **405**, 124228.

Dhanya, V. 2019 A statistical tool for the optimization of parameters for the degradation of mono-aromatic pollutants by a formulated microbial consortium. *Journal of Pure and Applied Microbiology* **13** (4), 2251–2260.

Duesterberg, C. K., Mylon, S. E. & Waite, T. D. 2008 pH effects on iron-catalyzed oxidation using Fenton's reagent. *Environmental Science and Technology* **42** (22), 8522–8527.

Fu, X. R., Gu, X. G., Lu, S. G., Sharma, V. K., Brusseau, M. L., Xue, Y. F., Danish, M., Fu, G. Y., Qiu, Z. F. & Sui, Q. 2017 Benzene oxidation by Fe(III)-activated percarbonate: matrix-consituent effects and degradation pathways. *Chemical Engineering Journal* **309**, 22–29.

Giannakis, S., Liu, S. T., Carratalà, A., Rtimi, S., Bensimon, M. & Pulgarin, C. 2017 Effect of Fe(II)/Fe(III) species, pH, irradiance and bacterial presence on viral inactivation in wastewater by the photo-Fenton process: kinetic modeling and mechanistic interpretation. *Applied Catalysis B: Environmental* **204**, 156–166.

Gligorovski, S., Strekowski, R., Barbati, S. & Vione, D. 2015 Environmental inplications of hydroxyl radicals (•OH). *Chemical Reviews* **115** (24), 13051–13092.

Godin, S., Kubica, P., Ranchou-Peyruse, A., Le Hecho, I., Patriarche, D., Caumette, G., Szpunar, J. & Lobinski, R. 2020 An LC-MS/MS method for a comprehensive determination of metabolites of BTEX anaerobic degradation in bacterial cultures and groundwater. *Water* **12** (7), 1869.

Hu, Y., Li, Y. L., He, J. Y., Liu, T., Zhang, K. S., Huang, X. J., Kong, L. T. & Liu, J. H. 2018 EDTA-Fe(III) Fenton-like oxidation for the degradation of malachite green. *Journal of Environmental Management* **226**, 256–263.

Huang, Z. J., Wu, P. X., Gong, B. N., Yang, S. S., Li, H. L., Zhu, Z. & Cui, L. H. 2016 Preservation of glutamic acid–iron chelate into montmorillonite to efficiently degrade Reactive Blue 19 in a Fenton system under sunlight irradiation at neutral pH. *Applied Surface Science* **370**, 209–217.

Huang, W. H., Dong, C. D., Chen, C. W., Surampalli, R. Y. & Kao, C. M. 2017 Application of sulfate reduction mechanisms for the simultaneous bioremediation of toluene and copper contaminated groundwater. *International Biodeterioration and Biodegradation* **124**, 215–222.

Huang, M., Wang, X. L., Liu, C., Fang, G. D., Gao, J., Wang, Y. J. & Zhou, D. M. 2020 Mechanism of metal sulfides accelerating Fe(II)/Fe(III) redox cycling to enhance pollutant degradation by persulfate: metallic active sites vs reducing sulfur species. *Journal of Hazardous Materials* **404** (Part B), 124175.

Jiang, W. C., Tang, P., Lyu, S. G., Brusseau, M. L., Xue, Y. F., Zhang, X., Qiu, Z. F. & Sui, Q. 2019 Enhanced redox degradation of chlorinated hydrocarbons by the Fe(II)-catalyzed calcium peroxide system in the presence of formic acid and citric acid. *Journal of Hazardous Materials* **368**, 506–513.

Jiang, F. C., Li, Y. L., Zhou, W., Yang, Z., Ning, Y., Liu, D. Q., Tang, Z., Yang, S., Huang, H. & Wang, G. W. 2020 Enhanced degradation of monochlorobenzene in groundwater by ferrous iron/persulfate process with cysteine. *Chemical Engineering Journal* **387**, 124048.

Khodaveisi, J., Banejad, H., Afkhami, A., Olyaie, E., Lashgari, S. & Dashti, R. 2011 Synthesis of calcium peroxide nanoparticles as an innovative reagent for in situ chemical oxidation. *Journal of Hazardous Materials* **192** (3), 1437–1440.

Li, T., Zhao, Z. W., Wang, Q., Xie, P. F. & Ma, J. H. 2016 Strongly enhanced Fenton degradation of organic pollutants by cysteine: an aliphatic amino acid accelerator outweighs hydroquinone analogues. *Water Research* **105**, 479–486.

Li, D., Zheng, T., Liu, Y. L., Hou, D., Yao, K. K., Zhang, W., Song, H. R., He, H. Y., Shi, W., Wang, L. & Ma, J. 2020 A novel electro-Fenton process characterized by aeration from inside a graphite felt electrode with enhanced electrogeneration of H_2O_2 and cycle of Fe^{3+}/Fe^{2+}. *Journal of Hazardous Materials* **396**, 122591.

Lu, S. G., Zhang, X. & Xue, Y. F. 2017 Application of calcium peroxide in water and soil treatment: a review. *Journal of Hazardous Materials* **337**, 163–177.

Lu, J., Wang, T. H., Zhou, Y., Cui, C. Z., Ao, Z. M. & Zhou, Y. B. 2020 Dramatic enhancement effects of l-cysteine on the degradation of sulfadiazine in Fe^{3+}/CaO_2 system. *Journal of Hazardous Materials* **383**, 121133.

Luo, L. S., Yao, Y. Y., Gong, F., Huang, Z. F., Lu, W. Y., Chen, W. X. & Zhang, L. 2016 Drastic enhancement on Fenton oxidation of organic contaminants by accelerating Fe(III)/Fe(II) cycle with L-cysteine. *RSC Advances* **6** (53), 47661–47668.

Ma, Y., Zhang, B. T., Zhao, L. X., Guo, G. S. & Lin, J. M. 2007 Study on the generation mechanism of reactive oxygen species on calcium peroxide by chemiluminescence and UV-visible spectra. *Luminescence* **22** (6), 575–580.

Ma, J., Yang, Y. Q., Jiang, X. C. H., Xie, Z. T., Li, X. X., Chen, C. Z. & Chen, H. K. 2018 Impacts of inorganic anions and natural organic matter on thermally activated persulfate oxidation of BTEX in water. *Chemosphere* **190**, 296–306.

Matta, R., Hanna, K. & Chiron, S. 2007 Fenton-like oxidation of 2,4,6-trinitrotoluene using different iron minerals. *Science of the Total Environment* **385** (1–3), 242–251.

Minetti, R. C. P., Macaño, H. R., Britch, J. & Allende, M. C. 2017 In situ chemical oxidation of BTEX and MTBE by ferrate: pH dependence and stability. *Journal of Hazardous Materials* **324**, 448–456.

Mosmeri, H., Gholami, F., Shavandi, M., Dastgheib, S. M. M. & Alaie, E. 2019 Bioremediation of benzene-contaminated groundwater by calcium peroxide (CaO_2) nanoparticles: continuous-flow and biodiversity studies. *Journal of Hazardous Materials* **371**, 183–190.

Munoz, M., de Pedro, Z. M., Casas, J. A. & Rodriguez, J. J. 2015 Preparation of magnetite-based catalysts and their application in heterogeneous Fenton oxidation – a review. *Applied Catalysis B: Environmental* **176–177**, 249–265.

Pan, Y., Su, H. R., Zhu, Y. T., Molamahmood, H. V. & Long, M. 2018 CaO_2 based Fenton-like reaction at neutral pH: accelerated reduction of ferric species and production of superoxide radicals. *Water Research* **145**, 731–740.

Qian, Y. J., Zhou, X. F., Zhang, Y. L., Zhang, W. X. & Chen, J. B. 2013 Performance and properties of nanoscale calcium peroxide for toluene removal. *Chemosphere* **91** (5), 717–723.

Qian, Y. J., Zhang, J., Zhang, Y. L., Chen, J. B. & Zhou, X. F. 2016 Degradation of 2,4-dichlorophenol by nanoscale calcium peroxide: implication for groundwater remediation. *Separation and Purification Technology* **166**, 222–229.

Ramos, M. D. N., Sousa, L. A. & Aguiar, A. 2020 Effect of cysteine using Fenton processes on decolorizing different dyes: a kinetic study. *Environmental Technology*, doi: 10.1080/09593330.2020.1776402.

Sarmento, A. P., Borges, A. C., de Matos, A. T. & Romualdo, L. L. 2016 Phenol degradation by Fenton-like process. *Environmental Science and Pollution Research* **23** (18), 18429–18438.

Stasik, S., Wick, L. Y. & Wendt-Potthoff, K. 2015 Anaerobic BTEX degradation in oil sands tailings ponds: impact of labile organic carbon and sulfate-reducing bacteria. *Chemosphere* **138**, 133–139.

Sun, Y., Lyu, S. G., Brusseau, M. L., Tang, P., Jiang, W. C., Gu, M. B., Li, M., Lyu, Y. C., Qiu, Z. F. & Sui, Q. 2019 Degradation of trichloroethylene in aqueous solution by nanoscale calcium peroxide in the Fe(II)-based catalytic environments. *Separation and Purification Technology* **226**, 13–21.

Sun, X. C., Sun, Y., Lyu, S. G., Qiu, Z. F. & Sui, Q. 2020 The performance of $nCaO_2$ for BTEX removal: hydroxyl radical generation pattern and the influences of co-existing environmental pollutants. *Water Environment Research* **92** (4), 622–630.

Tang, P., Jiang, W. C., Lyu, S. G., Qiu, Z. F. & Sui, Q. 2018 Ethanol enhanced carbon tetrachloride degradation in Fe(II) activated calcium peroxide system. *Separation and Purification Technology* **205**, 105–112.

Tang, S. F., Wang, Z. T., Yuan, D. L., Zhang, C., Rao, Y. D., Wang, Z. B. & Yin, K. 2020 Ferrous ion-tartaric acid chelation promoted calcium peroxide fenton-like reactions for simulated organic wastewater treatment. *Journal of Cleaner Production* **268**, 122253.

Wang, J. L. & Wang, S. Z. 2020 Reactive species in advanced oxidation processes: formation, identification and reaction mechanism. *Chemical Engineering Journal* **401**, 126158.

Xia, Y., Cheng, Y. P., Li, L. Y., Chen, Y. D. & Jiang, Y. P. 2020 A microcosm study on persulfate oxidation combined with enhanced bioremediation to remove dissolved BTEX in gasoline-contaminated groundwater. *Biodegradation* **31** (3), 213–222.

Xue, Y. F., Gu, X. G., Lu, S. G., Miao, Z. W., Brusseau, M. L., Xu, M. H., Fu, X. R., Zhang, X., Qiu, Z. F. & Sui, Q. 2016 The destruction of benzene by calcium peroxide activated with Fe(II) in water. *Chemical Engineering Journal* **302**, 187–193.

Xue, Y. F., Sui, Q., Brusseau, M. L., Zhang, X., Qiu, Z. F. & Lyu, S. G. 2018a Insight on the generation of reactive oxygen species in the CaO_2/Fe(II) Fenton system and the hydroxyl radical advancing strategy. *Chemical Engineering Journal* **353**, 657–665.

Xue, Y. F., Lu, S. G., Fu, X. R., Sharma, V. K., Mendoza-Sanchez, I., Qiu, Z. F. & Sui, Q. 2018b Simultaneous removal of benzene, toluene, ethylbenzene and xylene (BTEX) by CaO_2 based Fenton system: enhanced degradation by chelating agents. *Chemical Engineering Journal* **331**, 255–264.

Yang, Y., Pingnatello, J. J., Ma, J. & Mitch, W. A. 2014 Comparison of halide impacts on the efficiency of contaminant degradation by sulfate and hydroxyl radical-based advanced oxidation processes (AOPs). *Environmental Science and Technology* **48** (4), 2344–2351.

Yang, K. C., Ji, M., Liang, B., Zhao, Y. X., Zhai, S. Y., Ma, Z. H. & Yang, Z. F. 2020 Bioelectrochemical degradation of monoaromatic compounds: current advances and challenges. *Journal of Hazardous Materials* **398**, 122892.

Ye, J. P., Wang, S. Q., Zhang, P. Y., Nabi, M., Tao, X., Zhang, H. B. & Liu, Y. W. 2020 L-cysteine addition enhances microbial surface oxidation of coal inorganic sulfur: complexation of cysteine and pyrite, inhibition of jarosite formation, environmental effects. *Environmental Research* **187**, 109705.

Yuan, D. L., Zhang, C., Tang, S. F., Li, X., Tang, J. C., Rao, Y. D., Wang, Z. B. & Zhang, Q. R. 2019 Enhancing CaO_2 Fenton-like process by Fe(II)-oxalic acid complexation for organic wastewater treatment. *Water Research* **163**, 114861.

Zhang, A., Wang, J. & Li, Y. M. 2015a Performance of calcium peroxide for removal of endocrine-disrupting compounds in waste activated sludge and promotion of sludge solubilization. *Water Research* **71**, 125–139.

Zhang, X., Gu, X. G., Lu, S. G., Miao, Z. W., Xu, M. H., Fu, X. R., Qiu, Z. F. & Sui, Q. 2015b Degradation of trichloroethylene in aqueous solution by calcium peroxide activated with ferrous ion. *Journal of Hazardous Materials* **284**, 253–260.

Zhang, X., Gu, X. G., Lu, S. G., Brusseau, M. L., Xu, M. H., Fu, X. R., Qiu, Z. F. & Sui, Q. 2017 Application of ascorbic acid to enhance trichloroethene degradation by Fe(III)-activated calcium peroxide. *Chemical Engineering Journal* **325**, 188–198.

Zhao, B., Huang, F. Y., Zhang, C., Huang, G. X., Xue, Q. & Liu, F. 2020 Pollution characteristics of aromatic hydrocarbons in the groundwater of China. *Journal of Contaminant Hydrology* **233**, 103676.

Zheng, M., Daniels, K. D., Park, M., Nienhauser, A. B., Clevenger, E. C., Li, Y. M. & Snyder, S. A. 2019 Attenuation of pharmaceutically active compounds in aqueous solution by UV/CaO_2 process: influencing factors, degradation mechanism and pathways. *Water Research* **164**, 114922.

Zhou, Y. B., Fang, X. B., Wang, T. H., Hu, Y. H. & Lu, J. 2017 Chelating agents enhanced CaO_2 oxidation of bisphenol A catalyzed by Fe^{3+} and reuse of ferric sludge as a source of catalyst. *Chemical Engineering Journal* **313**, 638–645.

First received 24 March 2021; accepted in revised form 5 June 2021. Available online 17 June 2021